A new engineering approach to predict the hydrostatic strength of uPVC pipes

H.A. Visser (h.a.visser@ctw.utwente.nl, +31 53 4894346, University of Twente, the Netherlands)
T.A.P. Engels (Eindhoven University of Technology, the Netherlands)
L.E. Govaert (Eindhoven University of Technology, the Netherlands)
T.C. Bor (University of Twente, the Netherlands)

Abstract

Extruded unplasticised Poly(Vinyl Chloride) (uPVC) pipes are certified using pressurised pipe tests. During these tests the pipes are subjected to a certain temperature and internal pressure, while the time-to-failure, the time at which the internal pressure drops due to rupture or fracture, is measured. These tests are time consuming and are therefore costly. To circumvent these costs a model-based approach is proposed where the time-to-failure is predicted. The input parameters for this approach can be determined using short term measurements. The approach uses the observation that the time-to-failure kinetics of uPVC pipes subjected to an internal pressure is independent of the type of failure mode (ductile, semi-ductile or brittle). This supports our statement that the underlying mechanism that initiates failure is similar for these types of failure. Local deformation of the material up to a critical value of the anelastic strain is believed to determine the start of failure of the material. This critical strain appears to be constant for the testing conditions used during this study. A pressure modified Eyring expression is employed to calculate the strain rate resulting from the applied stress at a certain temperature. The time-to-failure follows from the calculated strain rate and the critical strain of the material. This approach has been verified against literature data and shown to hold quantitatively. Furthermore, the model seems to hold for different processing conditions.

1 Introduction

Polymer pipes have been in use for over fifty years in the field of gas and water distribution. A large part of these pipes is installed in rural areas, which imposes stringent demands on the safety as well as the life time of the pipes, as replacement is costly. Hence, thermoplastic pipes are commonly designed for a service life time of at least 50 years, which makes real time experiments for determining the maximum application stress unrealistic. Therefore, pressurised pipe tests (or burst tests) were developed for determining the long term hydrostatic strength (σ_{LTHS}) under accelerated conditions. ISO 1167 describes the procedure for carrying out these tests, where the pipes are subjected to predefined internal pressures and several temperatures, while the time-to-failure is measured. The long term hydrostatic strength can extrapolated according to ISO 9080 from the obtained data. Unfortunately pressurised pipe tests still last up to typically half a year. In combination with the spacious experimental setup required, this step in the certification process is costly. Therefore it is favourable to develop a method to predict the long term hydrostatic strength based upon short term measurements. Although this has been a scientific challenge for a long time, it still is relevant, proven by the fact that recently several studies were presented on this subject, like [1, 2] (for PE), [3] (for PVF_2) and [4] (for uPVC). In this case a new approach for uPVC pipes will be presented, which is unique in the sense that only the thermodynamic state of the pipe has to be known in order to predict its time-to-failure under internal pressure quantitatively.

1.1 Failure Mechanism

In 1959 Niklas et al. [6] presented pressurised pipe test data for uPVC pipes. Three different types of failure were distinguished for this material: ductile, semi-ductile and brittle. Four years later Niklas et al. [5] stated that the type of failure does not influence the failure kinetic of uPVC pipes during pressurised pipe test. This statement is based on the results as reproduced in figure 1, where the time-to-failure versus the applied stress is shown for uPVC pipe sections. The pipe sections were subjected to a temperature of 20°C, 40°C and 60°C, employing a range of internal pressures. Again the aforementioned three types of failure modes were recognized. Although there are distinct differences between the three types of failure, the failure kinetics appears to be identical. As noted by Niklas et al. [5] this suggests all three failure modes have one underlying failure mechanism. Based on an analysis of the development of the circumferential strain during these pressurised pipe test, they conclude that this underlying failure mechanism is the development of anelastic (or plastic) deformation up to a critical strain at which the pipe fails. This important observation seems to contradict the review of Lang et al. [7] published on life time prediction models for thermoplastic pipes under internal pressure. Lang et al. state that multiple aging processes (possible with different temperature rate dependence) occur simultaneously, although in some cases only one mechanism will be observed. Depending on the kinetics of these aging micro mechanisms this might or might not result in a change in the failure kinetics found experimentally with pressurised pipe tests, which will appear as a knee in the time-to-failure versus applied stress curve. For uPVC this existence of a knee (and thus multiple failure mechanisms) is still disputable. We believe that for a uPVC pipe that is properly stabilised the only limiting failure mechanism is the accumulation of anelastic strain up to a critical strain.

1.2 Critical strain

The short term experiments, upon which the predictions will be based, should give a measure for the anelastic deformation kinetics up to the critical strain of uPVC. For practical reasons tensile static

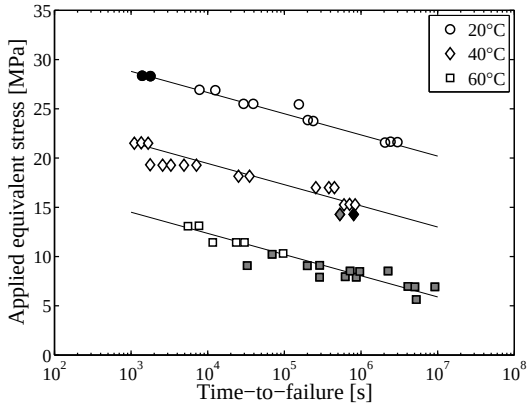

Figure 1: *Time-to-failure data originating from pressurised pipes tests on uPVC, as measured by Niklas et al. [5]. The unfilled, grey and black markers represent ductile, semi ductile and brittle failure respectively. The lines serve as guides to the eye.*

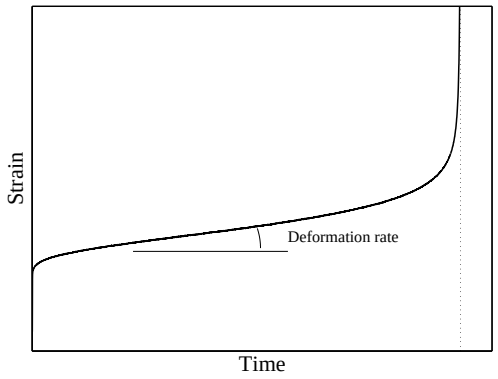

Figure 2: *Typical result of static fatigue tests as carried out in tension. The anelastic deformation rate is shown in the figure. The dotted line indicates where failure occurs.*

fatigue (creep) tests are chosen. These experiments are a one dimensional representation of what happens during burst tests. A typical result of a creep test is shown in figure 2. Upon loading the sample, it undergoes partly elastic and partly anelastic deformation. The anelastic part accumulates with a rate that can be calculated from the slope of the development of strain in time. Finally the polymer fails when the strain increases sharply within a short time frame (indicated by the dotted line in figure 2). Several approaches have been developed that use the concept of critical strain or cumulative damage and are capable to predict failure times for glassy polymers in (one dimensional) creep tests [8–12]. Although the concept is equivalent for these studies, the mechanisms causing the polymers to fail differs. We believe that strain softening is the origin of failure of uPVC pipes during burst tests. As Klompen et al. [13] state, strain softening causes a sharp increase in the strain during constant stress in both tension and compression. Although not noted, their results suggest a constant factor between the predicted strain rate and the time-to-failure: a critical value for the equivalent anelastic strain. This equivalent anelastic strain is believed to be the critical strain where the polymer (in this case PC) fails. The model in our approach calculates the development of equivalent anelastic strain until the critical value is reached. In contrast to aforementioned critical strain approaches, the model presented in this paper is capable of describing three dimensional loading cases.

1.3 Analogy between tensile and creep tests

Ogorkiewicz et al. [14] state that the results of tensile tests at constant strain and tensile tests at constant stress (creep tests) on uPVC are interchangeable; the data obtained under one set may be used to predict results under other conditions for the other set. The same has been found for PC ([15]) and PMMA ([16]). As a result the anelastic deformation rate during creep experiments can be predicted using yield stress data at several strain rates. The approach presented here uses this observation for predicting the failure time during pressurised pipe tests based on tensile yield stress data of uPVC.

1.4 Model

There have been several successful attempts in the past to predict the deformation kinetics (mostly yield stress versus strain rate and temperature) of polymers. In most cases, like in [17–20], modifications of the equation for the viscosity of non-Newtonian flows as proposed by Eyring [21] and Ree-Eyring [22] are used. In these cases the model was restricted to one dimensional loading cases. Klompen et al. [13] used a pressure modified Eyring type equation to relate the equivalent strain rate ($\dot{\bar{\gamma}}$) with the applied equivalent shear stress ($\bar{\tau}$). By incorporating the influence of the hydrostatic pressure (P_h), the relation holds for different loading cases and geometries, while using

	Definition	Tensile	Pressurised pipe
$\dot{\bar{\gamma}}$=	$\sqrt{2\mathrm{tr}\left(\dot{\boldsymbol{\epsilon}}\cdot\dot{\boldsymbol{\epsilon}}\right)}$	$\sqrt{3}\dot{\epsilon}$	
p=	$-\frac{1}{3}\mathrm{tr}\left(\boldsymbol{\sigma}\right)$	-$\frac{1}{3}\sigma$	$-\frac{(\mathrm{D}-\mathrm{t})\mathrm{p_i}}{4\mathrm{t}}$
$\bar{\tau}$=	$\sqrt{\frac{1}{2}\mathrm{tr}\left(\boldsymbol{\sigma_s^d}\cdot\boldsymbol{\sigma_s^d}\right)}$	$\frac{\sigma}{\sqrt{3}}$	$\frac{(\mathrm{D}-\mathrm{t})\mathrm{p_i}}{4\mathrm{t}}$

Table 1: *Definition of equivalent strain rate and stresses, including the resulting relations for tensile and pressurised pipe tests, where $\boldsymbol{\sigma_s^d}$ is equal to the product of the shear modulus and the deviatoric part of the isochoric elastic left Cauchy-Green strain tensor.*

only one parameter set. This model is capable of describing deformation kinetics of pressurised pipes, as the stresses in this loading case can be translated into an equivalent stress.

$$\dot{\bar{\gamma}}\left(\mathrm{T},\bar{\tau},\mathrm{p}\right)=\dot{\bar{\gamma}}_0\cdot\exp\left(\frac{-\Delta U_a}{R\cdot T}\right)\cdot\exp\left(\frac{-\mu\cdot p\cdot\bar{V}^*}{k\cdot T}\right)\cdot\sinh\left(\frac{\bar{\tau}\cdot\bar{V}^*}{k\cdot T}\right) \tag{1}$$

The three material parameters that can be recognised in this equation are the activation energy for temperature induced deformation ($\Delta\mathrm{U_a}$), the activation volume defining the stress induced deformation ($\bar{\mathrm{V}}^*$) and the dimensionless pressure dependence (μ). The thermodynamic state of the polymer is defined by the zero strain rate ($\dot{\bar{\gamma}}_0$). The definitions for the equivalent strain rate ($\dot{\bar{\gamma}}$), hydrostatic pressure (p) and equivalent shear stress ($\bar{\tau}$) are given in table 1, as well as the resulting relation for tensile and pressurised pipe tests.

The time-to failure for a geometry that undergoes a constant deformation rate (as a result of a constant applied stress at constant temperature) can be calculated with:

$$t_f=\frac{\bar{\gamma}_{cr}}{\dot{\bar{\gamma}}\left(\mathrm{T},\bar{\tau},\mathrm{p}\right),} \tag{2}$$

where $\bar{\gamma}_{\mathrm{cr}}$ is the equivalent critical strain. Combining equations (1) and (2) and using the approximation that $\sinh(x)\approx\frac{1}{2}\exp(x)$ for $\gg>1$, gives the time to failure for a static fatigue test as measured in tension:

$$t_f\left(\mathrm{T},\sigma\right)=\frac{2\bar{\gamma}_{cr}}{\dot{\bar{\gamma}}_0}\cdot\exp\left(\frac{\Delta U_a}{R\cdot T}-\frac{\left(\mu+\sqrt{3}\right)\bar{V}^*}{3k\cdot T}\cdot\sigma\right) \tag{3}$$

2 Experimental

2.1 Material and sample preparation

The uPVC samples are taken out of an excavated uPVC gas distribution pipe (∅ 160 mm) that had been in service for several years. With a bandsaw a 70 mm long part is cut from the pipe material. This part is sawed in axial direction, resulting in two semi-cylindrical parts. These pieces were pressed into flat plates in a press at 100°C. Tensile bars with a parallel gauge section of approximately 30×5×4 mm^3 were milled from the plate material. To prevent a significant contribution of physical aging during the experiments at elevated temperatures, the samples were annealed for $5\cdot10^5$ s at 60°C in a convection oven prior to testing.

2.2 Mechanical testing

All uniaxial tensile and static fatigue measurements were carried out on a MTS Elastomer Testing System 810 equipped with a 25 kN force cell and an environmental chamber. The tests were conducted at three different temperatures (20°C, 40°C and 60 °C). The engineering stresses are calculated using the average of the cross sectional surface areas as measured at three locations in the gauge length. Tensile experiments were carried out at a constant crosshead speed, thus at engineering strain rate. The static fatigue tests were conducted with a constant load, thus at constant engineering stress. All stresses and strains in this paper are engineering values.

	[23]	Current study	
$\bar{\mathrm{V}}^*$	3.22	3.42	[nm^3]
$\Delta \mathrm{U_a}$	295	297	[kJ·mol^{-1}]
μ	-	0.14	[-]
$\bar{\gamma}_{\mathrm{cr}}$	-	0.015	[-]

Table 2: *Material parameters for uPVC. The parameters as determined in [23] for their model were translated into equivalent parameters for our model using μ=0.14.*

2.3 Deformation kinetics

The deformation kinetics are determined by material parameters $\bar{\mathrm{V}}^*$, $\Delta \mathrm{U_a}$ and μ and the thermodynamic state of the material, which is represented with $\dot{\bar{\gamma}}_0$. These parameters are determined by fitting (1)on yield data from tensile tests. The pressure dependence is determined from yield data resulting from tensile test with a superimposed hydrostatic pressure (p). The pressure dependence can be calculated from the slope of the yield stress versus the superimposed hydrostatic pressure.

$$\frac{\mathrm{d}\sigma}{\mathrm{d}p} = \frac{3\mu}{\mu + \sqrt{3}} \tag{4}$$

Using data yield data as measured by Yuan et al. [24] (shown in figure 3) the pressure dependence of uPVC turns out to be 0.14. The results of tensile yield stress measurements at various strain rates and temperatures for uPVC as carried out during this study is shown in figure 4. The solid lines represent best fit of (1) and describe the results in yield data very well. Moreover, the parameter set obtained from the least squares fit on the experimental data, agrees with the parameter set as determined by Bauwens-Crowet et al. [23] within experimental error (see table 2).

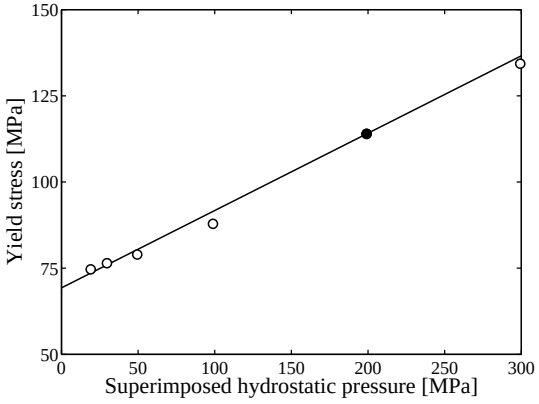

Figure 3: *The yield stress of uPVC as measured in tension with a superimposed hydrostatic pressure as measured by Yuan et al. [24]. The solid line is a fit using (4) and $\mu = 0.14$.*

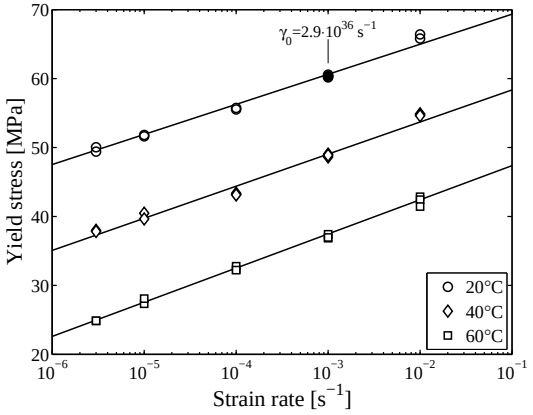

Figure 4: *Tensile yield stress of uPVC for various strain rates at three temperatures. The solid lines represent the best fit using (1)*

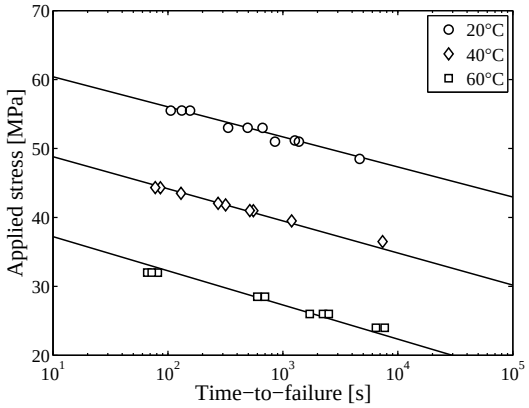

Figure 5: *Results of tensile static fatigue experiments on uPVC at three temperatures. The solid lines represent the best fit of the model using the critical strain as the fit parameter*

2.4 Determining the critical strain

The time-to-failure as measured for various applied stresses at three temperature levels is shown in figure 5. The solid lines represent the fit using equation 3 and an equivalent critical strain value of 1.5%. The model appears to take influence of temperature and stress appropriately into account. To investigate the predictive value of the approach for different situations, it is validated on samples with different physical states. Conclusively the approach will be validated for the goal of this research: to predict the long term hydrostatic stress of pipes by comparing the model predictions with results of pressurised pipe tests.

2.5 Model validation

In order to validate the model for uPVC structures with a different physical state, some samples were annealed for $3 \cdot 10^6$ s at 60°C. The deformation kinetics of these samples are compared with that of the samples used to determine the material parameters. These samples received a shorter annealing treatment and will therefore differ in thermodynamic state. The results of tensile and static fatigue tests can be found in figures 6 and 7, respectively. The zero strain rate, $\dot{\bar{\gamma}}_0$, is determined using the yield stress at a strain rate of 10^{-3} s^{-1}. The model is capable of predicting the time-to-failure for both thermodynamic states correctly.

2.6 Predicting the σ_{LTHS} for uPVC pipes

To conclude the validation of the model it is used to predict the results of pressurised pipe tests. The stress state in the pipe is given by the stress in the circumferential (referred to as hoop stress, σ_{h}), longitudinal (σ_{l}), and the radial direction (σ_{r}). In a pressurised pipe test, where a constant internal pressure ($\mathrm{p_i}$) is applied, these stresses can be calculated using Barlow's formula for thin-walled pressure vessels:

$$\begin{aligned} \sigma_h &= \frac{(D-t)p_i}{2t}, \\ \sigma_l &= \frac{(D-t)p_i}{4t}, \\ \sigma_r &= 0, \end{aligned} \tag{5}$$

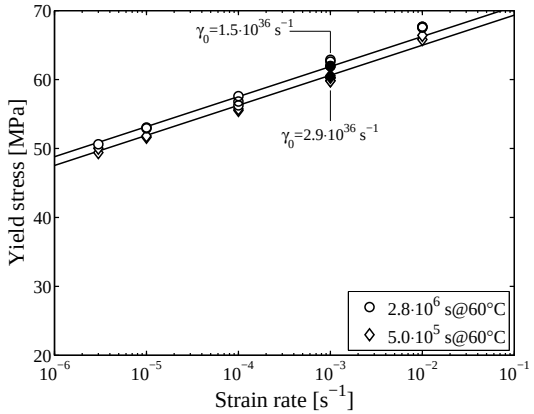

Figure 6: *Engineering yield stress versus strain rate measured at a temperature of 20^{o}C for uPVC samples with different thermal histories.*

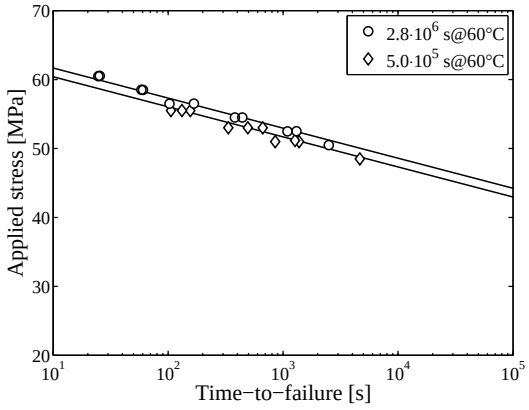

Figure 7: *Time-to-failure versus the applied stress as measured with tensile static fatigue test at 20^{o}C for uPVC samples with different thermal histories*

with D, the outer diameter of the pipe and t, the wall thickness. In some cases the pipes are sealed with special fittings instead of end caps, preventing the pipe from being loaded in the longitudinal direction (σ_l=0). In the analysis that follows, the use of end caps is assumed.

Combining (1), (2) and (5) and again using the approximation that $\sinh(x) \approx \frac{1}{2}\exp(x)$ for $x \gg 1$ results in the following relation for the time-to-failure of pressurised pipe test.

$$t_f\left(\mathrm{T}, \mathrm{p_i}\right) = \frac{2\bar{\gamma}_{cr}}{\dot{\bar{\gamma}}_0} \cdot \exp\left(\frac{\Delta U_a}{R \cdot T} - \frac{(1+\mu)\,(D-t)\,\bar{V}^*}{4t \cdot k \cdot T} \cdot p_i\right) \tag{6}$$

Niklas et al. [5] presented their data in the form of Von Mises stress (σ_{vm}) versus time-to-failure. The

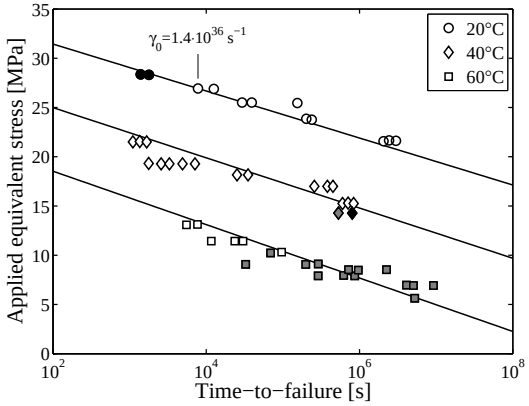

Figure 8: *Time-to-failure data originating from pressurised pipes tests on uPVC, as measured by Niklas et al. [5]. The unfilled, grey and black markers represent ductile, semi ductile and brittle failure respectively. The solid lines are predictions using equation 6.*

Von Mises stress during a pressurised pipe test is given by:

$$\sigma_{vm} = \sqrt{3}\frac{(D-t)\,p_i}{4t}, \tag{7}$$

thus $\sigma_{\mathrm{vm}} = \sqrt{3}\bar{\tau}$. Therefore the data of Niklas et al. can be predicted without the knowledge of the diameter and wall thickness of the pipes used. To compare the results of Niklas et al. with the predictions of the presented model, the thermodynamic state of the samples has to be known. The zero strain rate is calculated using one data point as a reference point as indicated in figure 8 ($\dot{\bar{\gamma}}_0$=1.4·10^{36} s^{-1}). This value of the zero strain rate a yield stress of 60.4 MPa is predicted for a tensile test at a strain rate of 10^{-3} s^{-1} at room temperature, which is a realistic value for a tensile test on uPVC. The solid lines in figure 8 represent the model prediction using the material parameters as derived during the current research and the zero strain rate corresponding to the reference point indicated in the figure. Not only the slope of the data points is predicted accurately, but also the influence of the temperature agrees very well with the experimental values. The measurements conducted at 20^{o}C show little scatter. The prediction for the time-to-failure at this temperature is in good agreement with the measured data. At higher temperature the scatter increases, which clouds the quality of the predictions.

3 Discussion

All uPVC pipes are produced using the extrusion process. The processing conditions have a great influence on the quality of the the pipe. Firstly the thermodynamic state of the pipe depends on the process temperature and the cooling of the pipe after extrusion. Furthermore, the processing parameters determine the level of gelation in the uPVC pipe. In this section the influence of these two processing effects on the quality of the model predictions will be discussed.

3.1 Influence of physical aging

A slowly cooled uPVC pipe will have a different thermodynamic state than one that is cooled rapidly. Therefore the zero strain rate has to be determined using one data point for each batch of samples. But during the tests the thermodynamic state of the pipe can change as well, which is commonly referred to as physical aging [25]. Klompen et al. [13] observed a fatigue limit for PC at long term loading cases, as a result an increased resistance against anelastic deformation, due to physical aging. At this fatigue limit the time-to-failure appears to be nearly independent of the applied stress.

The presented model does not incorporate physical aging, as the value of $\dot{\bar{\gamma}}_0$ is kept constant for a set of samples. The process of physical aging is accelerated at elevated temperatures as well as by applying stress. Both temperature and stress increase the mobility of the polymer chains. Consequently, the chains will move faster towards their thermodynamic equilibrium, resulting in accelerated aging. Nonetheless, the effect is not as strong in figure 8 as one would expect. A possible explanation is that the samples used in [5] were already aged quite a bit prior to testing. The relatively high predicted tensile yield stress of 60.4 MPa supports this explanation. Currently the aging kinetics of uPVC are under investigation, to find out if there are other mechanisms taking place which compensate for the increased deformation resistance during the pressurised pipe tests at elevated temperatures.

3.2 Influence of the level of gelation

As stated already, 10% of the structure of PVC is crystalline. The melting temperature of these regions is above the thermal degradation temperature of PVC. This makes the compounding of PVC a difficult process and therefore uPVC pipes are processed directly from uPVC powder instead of compounded granules. By applying high shear forces at temperatures where the thermal degradation is acceptable, the primary structure of the powder particles is destroyed. The operating window for uPVC extrusion is very small and thus a difficult process to control. The level of gelation, which is the degree of destruction of the primary structure, has a significant influence on the properties of the uPVC pipe. The approach is based on well gelated uPVC pipe material. Although the yield stress is not insensitive to changes in the level of gelation, the short-term burst strength does appear to be sensitive [26]. An uPVC pipe material with a level of gelation of around 60% has a lower strength than those with a gelation level of around 90%. The failure kinetics during long-term pressurised pipe tests does not seem to be affected by the level of gelation [27, 28]. The failure mode does change however, as for lower gelation levels brittle failure occurs on shorter time scales.

These observations suggest that the approach holds for various processing conditions, although further research is needed to confirm this statement.

4 Conclusions

A new engineering approach for predicting the long term hydrostatic strength for polymer pipes based on short term experiments is presented. The model is applied on both PC and uPVC and shown to hold quantitatively for different load cases and different thermodynamic states. The approach neglects the occurrence of physical aging during the time frame of the pressurised pipe experiments and is developed on uPVC pipe material with a high level of gelation. Nevertheless, this does not seem to be a limitation for the validity of the model for different process conditions.

Acknowledgements

The authors gratefully acknowledge the financial support provided by four Dutch gas distribution network providers: Cogas Netbeheer, Continuon, Eneco Netbeheer and Essent Netwerk.

References

[1] N. Brown. *Polymer Engineering and Science*, 47:477–480, 2007.

[2] G. Pinter et al. *Monatshefte fur Chemie*, 138:347–355, 2007.

[3] S. Castagnet et al. Consequences of annealing during long-term pressure tests on polyvinylidene fluoride pipes. In *Proceedings of Plastic pipes XII*, 2004.

[4] G. Castiglioni et al. Prediction of ductile failure in u-pvc pipes from creep tests on specimens. In *Proceedings of Plastic pipes XII*, 2004.

[5] H. Niklas and H.H. Kausch von Schmeling. *Kunststoffe*, 53:886–891, 1963.

[6] H. Niklas and K. Eifflaender. *Kunststoffe*, 49:109–113, 1959.

[7] R.W. Lang et al. *Die Angewandte Makromolekulare Chemie*, 247:131–145, 1997.

[8] B.D. Coleman. *Journal of Polymer Science*, 20:447–455, 1956.

[9] S.N. Zhurkov. *International Journal of Fracture Mechanics*, 1:311–323, 1965.

[10] C. Bauwens-Crowet et al. *Journal of Materials Science Letters*, 4:1197–1201, 1974.

[11] G.B. McKenna and R.W. Penn. *Polymer*, 21:213–220, 1980.

[12] J.M. Crissman and G.B. McKenna. *Journal of Polymer Science Part B: Polymer Physics*, 28:1463–1473, 1990.

[13] E.T.J. Klompen et al. *Macromolecules*, 38:6997–7008, 2005.

[14] R.M. Ogorkiewicz and A.A.M. Sayigh. *British Plastics*, 40:126–128, 1967.

[15] M.J. Mindel and N. Brown. *Journal of Materials Science*, 8:863–870, 1973.

[16] O.D. Sherby and J.E. Dorn. *Joural of the Mechanics and Physics of Solids*, 6:145–162, 1958.

[17] J.-C. Bauwens. *Journal of Polymer Science: Part A-2*, 5:1145–1156, 1967.

[18] R.E. Robertson. *Journal of Applied Polymer Science*, 7:443–450, 1963.

[19] E. Pink. *Materials Science and Engineering*, 22:85–89, 1976.

[20] Y. Nanzai. *Progress in Polymer Science*, 18:437–479, 1993.

[21] H. Eyring. *Journal of Chemical Physics*, 4:283–291, 1936.

[22] T. Ree and H. Eyring. *Journal of Applied Physics*, 26:794–800, 1955.

[23] C. Bauwens-Crowet et al. *Journal of polymer science. Part A-2, Polymer Physics*, 7:735–742, 1969.

[24] J. Yuan et al. *Journal of Materials Science*, 18:3063–3071, 1983.

[25] L.C.E. Struik. *Physical aging in amorphous polymers and other materials*. Elsevier, 1978.

[26] M. Moghri et al. *Journal of Vinyl & Additive Technology*, 9:81–89, 2003.

[27] P. Benjamin. *Journal of Vinyl Technology*, 2:254–258, 1980.

[28] J. Bystedt et al. *Journal of Vinyl Technology*, 10:100–102, 1988.